Three-Dimensional Monte-Carlo/Particle-in-Cell studies of anode striations and cathode ionization wave in barrier-discharges in AC-PDP cell

A. Shvydky, V.N. Khudik, V.P. Nagorny, and C.E. Theodosiou

***Abstract*—The dynamics of the sustain discharge pulse in an AC-PDP cell is studied via the 3-D PIC-MC simulations. Key phases in the discharge development are identified and thoroughly illustrated with an extensive set of plots. The main effort is focused on the study of the striations above the dielectric surface of the anode and on understanding the mechanisms responsible for the propagation of the cathode ionization wave. Both of these phenomena are representative examples of dielectric-surface charging processes in strongly collisional plasmas of barrier discharges.**

***Index Terms*—Plasma display panels, PDP, three-dimensional particle-in-cell simulations, Monte-Carlo simulations, striations, cathode fall, ionization wave.**

I. INTRODUCTION

PLASMA Display Panels (PDPs) has been know for almost 40 years since their invention in 1966 by Bitzer and Slottow [1, 2]. Nowadays PDP is a mature technology with a substantial market share, and PDP TVs are widely commercially available. The advantage of PDP televisions as compared to regular cathode-ray-tube (CRT) and projection TVs is their thinness (about 5in) and as compared to liquid-crystal-displays (LCDs) is their picture quality – very high contrast ratio and wide viewing angles. At the same time, there are still some problems (most significant of which are the low efficiency and high cost) that prevent PDPs from dominating the market. Efforts of many scientists and engineers from both industry and academia aimed at solving these problems continue to generate a steady stream of research related to PDPs (see, for example, [3-7]).

A typical alternating-current (AC) PDP consists of two flat, square pieces of glass - front plate and back (or rear) plate (see Fig.1). The front plate has a large number (typically from 480 to 853 depending on whether the panel is a regular or High-Definition TV) of pairs of transparent “sustain” electrodes, running in the horizontal direction, printed onto the glass surface and covered with about 40μm thick layer of dielectric. A thin (about 500nm) layer of MgO is then deposited on top of the dielectric layer. The back plate has even greater number of “address” electrodes (one for each red, green, and blue colors times the number of pixels in the horizontal direction - 640 up to 1366 depending on the type of the TV panel) running in the vertical direction. The address electrodes are printed onto the back plate and are covered with the dielectric layer. Next, the barrier ribs (of about 60-80μm in width and 100-150μm in height) are sandblasted on top of the dielectric layer between the address electrodes. Facing each other sides of adjacent barrier ribs and the surface of the dielectric between them are then covered with the phosphor material. The back and front plates are brought together (with electrode surfaces facing each other) and sealed around the perimeter, after which the system is evacuated and filled with the mixture of Ne and Xe gases (with 4-10% of Xe) at a pressure of about 500Torr.

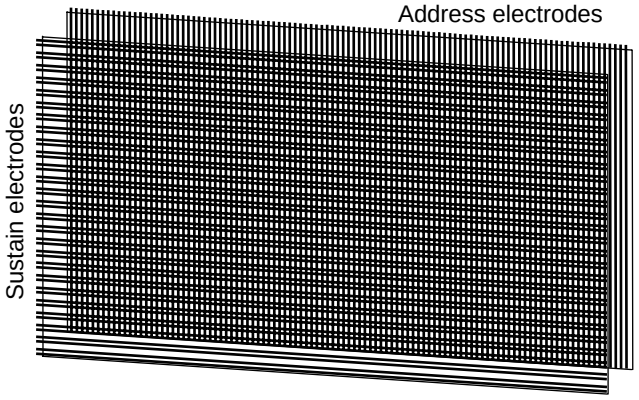

Fig. 1. PDP electrode schematics.

The volume encompassed by a pair of adjacent barrier ribs and a pair of sustain electrodes constitutes one cell (outlined in Fig.2). Applying voltages to the electrodes causes the discharge within a cell. The UV radiation produced by the discharge excites the phosphor, which in turn emits the red, green, or blue light (depending on the phosphor type). By lighting up some cells while turning off the others, a TV image is reproduced. In order to be able to selectively light up an arbitrary cell, one has to use quite sophisticated voltage waveforms (sometimes called “driving schemes”) applied to sustain and address electrodes [3].

Since the electrodes are covered with dielectric layers, the only way to sustain the discharge in the AC-PDP is by using an AC voltage. All the driving schemes are based on

Manuscript received October 14, 2005.

A. Shvydky and C.E. Theodosiou are with the Department of Physics and Astronomy, University of Toledo, Toledo, OH 43606 USA (e-mail: ashvidk@physics.utoledo.edu).

V.N. Khudik and V.P. Nagorny are with Plasma Dynamics Corp., 1004 Waterville-Monclova Rd., Waterville, OH 43566 USA.

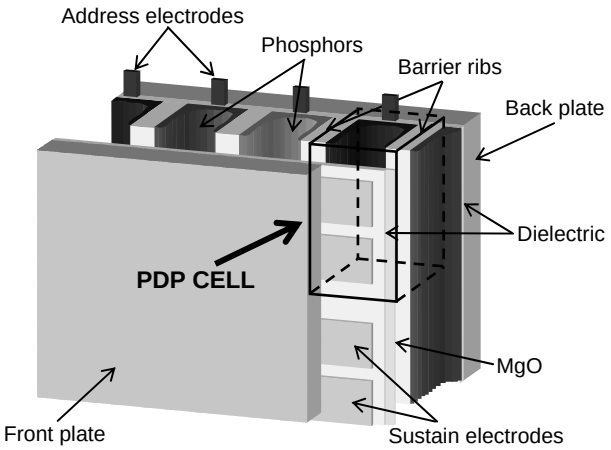

Fig. 2. PDP design.

the so called bi-stability effect [8] of the barrier discharge - a property of the barrier discharge to be ON or OFF, while driven with the *same* periodic square-wave voltage, depending on whether or not there is a charge on the dielectric surface prior to applying the driving voltage: If the charge is zero, applying to the cell a square-wave voltage of the amplitude lower than the breakdown voltage does not cause the breakdown, and the cell stays OFF (i.e. no discharges occur in the cell). But, if before applying the voltage there is a certain amount of charge on the dielectric surfaces, the electric field created by this charge will increase the electric field due to external voltage and cause the breakdown, turning the cell ON (i.e. discharges occur in the cell at each half-cycle of applied voltage).

Any of the currently used driving waveforms always contains the address and sustain parts: During the address part, the cells that are intended to be ON are "written" by applying a voltage between the address and one of the sustain electrodes of the desired cells and triggering the discharge that deposits the charge onto the dielectric surfaces. During the following sustain part, a square-wave periodic voltage is applied to sustain electrodes of all cells in the panel. Only cells that were written turn ON and emit light. The frequency of sustain waveform is 100-200 kHz and the voltage is 170-250 V, depending on the cell geometry and gas mixture.

In Fig. 3 are shown the top and side views of a coplanar AC-PDP cell. The typical dimensions of the cell are of the order of 100μm and are much larger than the electron mean free path which is about 1μm (for traditionally used gas pressures and compositions), so that the plasma created during a PDP discharge is highly collisional. But since the electron energy equilibration length due to elastic collisions ($\lambda_\varepsilon \sim (M/m)^{1/2}\,\lambda \sim 200\mu m$, where M is the mass of the atoms of the background gas and m is the electron mass; see [9]) is comparable to the cell size, the electron energy distribution function is quite far from the equilibrium and therefore non-local effects (of which the striations are the most notable) readily occur.

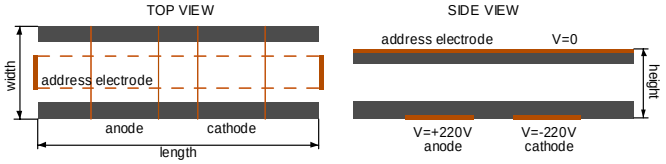

Fig. 3. Geometry of a standard coplanar cell.

In this paper, via 3- and 2-dimensional PIC/MC simulations we study the discharge during a single sustain pulse. Specific attention is paid to the striations over the anode and the cathode fall (CF) spreading (cathode ionization wave propagation) over the cathode. The paper is based on our previous work [10-12] and organized as follows: In Section II, a brief description of the Particle-in-Cell/Monte-Carlo algorithm is presented. In Section III, the general phases of the discharge development during a single sustain pulse are described. In Section IV, we consider the anode striation phenomena and present a series of specifically designed experiments aimed to clarify the phenomena. In Section V, we study the spreading of the dynamic cathode fall above the cathode dielectric surface.

II. PARTICLE-IN-CELL/MONTE-CARLO ALGORITHM

Starting from the values of applied voltage and the dielectric layer capacitance, one can easily estimate that the number of charged particles transferred during one discharge pulse in a typical PDP cell is of the order of 10^8. On the other hand, the number of macro-particles in typical Monte-Carlo/PIC simulations that can run on a modern PC is about several millions. It means that one positive/negative macro-particle can be taken to correspond to only several tens of real ions/electrons, and therefore, 3-D Monte-Carlo/PIC simulations of a PDP cell are quite realistic. Parallelizing the code enables one to run the simulations on, nowadays widespread, computer clusters with tens and hundreds of processors, which allows following each charged particle individually (i.e. when one meta-particle corresponds to one real ion/electron)! This as well as special care taken to avoid the numerical heating makes the simulations able to correctly treat statistical fluctuations – important, for example, for analysis of weak discharges with small numbers of charged particles.

The speed advantage of the PIC/MC method comes from the simple fact that the electron distribution function in the Boltzmann equation is defined in a 6-dimensional space, and its discretization with any reasonable accuracy would require manipulation with huge arrays (with, at least, 10^9-10^{10} elements), even if there are only a few electrons in the PDP cell. On the other hand, one can limit the number of particles in PIC/MC simulations to several millions, which results in a speed advantage of about 10^3.

In our simulations each macro-particle corresponds to 50 electrons/ions, and the total number of particles in the PDP cell does not exceed four million. The algorithm that we use is similar to [13]. In order to accurately reproduce the electron trajectories and resolve the collision times, electrons are

advanced with a time step of less than 10^{-5} ns. To simulate the electron collisions, we use a null-collision technique with a set of cross-sections similar to [14]. Cross-sections for ion collisions are from [15]. The standard chemical model of Xe/Ne mixture discharge [14, 16] has been used to follow the evolution of the excited species. The Poisson equation for the electric potential is solved on a 3-D rectangular mesh with a cell size of about several microns using a combination of the FFT and the "capacitance matrix" [13] methods.

In order to obtain the bounds on the time step Δt for recalculating the electric potential let us consider the equations of the fluid model in which the inertia of electrons is taken into account [9]:

$$m n_e \frac{d\mathbf{v}}{dt} = -e n_e \mathbf{E} - m\nu_m (n_e \mathbf{v} + D_e \nabla n_e), \qquad (1)$$

$$\frac{\partial n_e}{\partial t} = -div(n_e \mathbf{v}), \qquad (2)$$

$$div\mathbf{E} = \frac{e}{\varepsilon_0}(n_i - n_e), \qquad (3)$$

where $\mathbf{v}$ is the electron velocity, n_e is the electron density, m is the electron mass, e is the electron charge, ν_m is the momentum transfer collision frequency, and D_e is the electron diffusion coefficient. Since slow ions do not impose additional limitations on the time step Δt, the ion density is taken constant, $n_i = n_0$.

Let us consider evolution of small perturbations of the electron density in the uniform plasma of density n_0: $n_e = n_0 + n'$ ($n' << n_0$). From (1) – (3), it follows

$$\frac{\partial^2 n'}{\partial t^2} + \nu_m \frac{\partial n'}{\partial t} - \nu_m D_e \nabla^2 n' = -\omega_{pe}^2 n', \qquad (4)$$

where $\omega_{pe} = \left(e^2 n_0 / \varepsilon_0 m\right)^{1/2}$ is the electron plasma frequency. Leaving the dispersion effects for a more rigorous analysis, we omit the diffusion term (proportional to $\nabla^2 n'$) in Eq. (4) and find the following expression for the frequency ω of the natural oscillations ($\sim \exp(-i\omega t)$):

$$\omega_{1,2} = -\frac{i}{2}\nu_m \mp \sqrt{\omega_{pe}^2 - \frac{1}{4}\nu_m^2}. \qquad (5)$$

In the case of a strongly collisional plasma ($\nu_m >> \omega_{pe}$), we obtain $\omega_1 \approx -i\nu_m$ and $\omega_2 \approx -i\omega_{pe}^2 / \nu_m$. The first eigenmode is related to the relaxation of the electron momentum due to collisions, and it is reproduced in our numerical algorithm by advancing the electrons with a time step ($\sim 10^{-14}$s) much less than ν_m^{-1} (which is about 10^{-12}s for a gas mixture used in simulations). The second mode is reproduced in our numerical algorithm by recalculating the Poisson equation with a time step $\Delta t < \tau_m$, where $\tau_m \equiv \nu_m / \omega_{pe}^2$ is the electron Maxwellian time. Note that in the case of a strongly collisional plasma the time step Δt can be taken much greater than ω_{pe}^{-1}.

In the opposite case of a weakly collisional plasma ($\nu_m << \omega_{pe}$), the frequencies of the natural oscillations $\omega_{1,2} \approx \mp\omega_{pe}$. In order to suppress the artificial numerical heating of electrons for an extended period of time, one must take the time step Δt at least less than $0.2\omega_{pe}^{-1}$ (the smaller the numerical coefficient the less the artificial heating [17]). It is useful to note that ω_{pe} becomes comparable with $\nu_m \sim 10^{12} s$ at quite a high density of the plasma $n_0 \sim 3 \cdot 10^{14} cm^{-3}$.

While in the general case one can use the expression (5) to get a limitation on the time step, for the sake of simplicity we incorporated into the numerical algorithm the following formula for the time step: $\Delta t = (\omega_{pe}^{-1} + \tau_m)/K$, where a numerical coefficient $K >> 1$, and ω_{pe}^{-1} and τ_m are evaluated at a point in the volume with the maximum plasma density.

When using standard PIC/MC algorithms for simulating discharges in PDPs, special attention should be paid to the artificial heating. The duration of the afterglow is up to 1μs which is about 10^6 times greater than ω_{pe}^{-1}, which means that the code should be able to reproduce that many plasma periods without causing the artificial heating. The standard (explicit) PIC codes that are based on leap-frog or Verlet algorithms, while being good for thousands of time steps, are inadequate for the simulation of the full sustain pulse. Fortunately, in most of the sustain PDP discharges the plasma density is not very high and the plasma frequency almost never exceeds the electron collision frequency, i.e. $\omega_{pe} \le \nu_m$. Intuitively it is clear that under such conditions it is much more important to "conserve" the electron energy during the time step than to accurately reproduce the actual electron trajectory. After many trials and errors we found an empirical algorithm (details of which will be presented elsewhere) that exceptionally well suppresses the artificial heating at not too high plasma densities, and is capable of reproducing the electron cooling due to elastic collisions. The idea is based on introducing a correction to the kinetic energy of electrons, after pushing them in the old electric field, using the values of the new electric field.

III. DYNAMICS OF SUSTAIN DISCHARGE PULSE IN PDP CELL

In this section we describe general features of a sustain discharge pulse in an AC-PDP cell which weakly depends on the specifics of discharge parameters [10]. We consider a standard coplanar PDP cell, filled with neon-xenon (93% - 7%) mixture at a pressure of 500 Torr. The cell length, width, and height are 650μm, 220μm (including barrier ribs), and 160μm (including dielectric layers above sustain and address electrodes with dielectric permeability equal to 11), respectively (see Fig.3). The distance between sustain electrodes is 90μm, the sustain electrode width is 155μm, and the voltage applied to the sustain electrodes is $\pm$220V. The secondary electron emission coefficients for Ne and Xe ions are 0.5 and 0.01, respectively.

Since the distance between sustain electrodes is small, the barrier discharge in AC-PDP cell develops mainly near the

dielectric surface above the anode and the cathode. It goes through the following stages (illustrated in Fig.4)

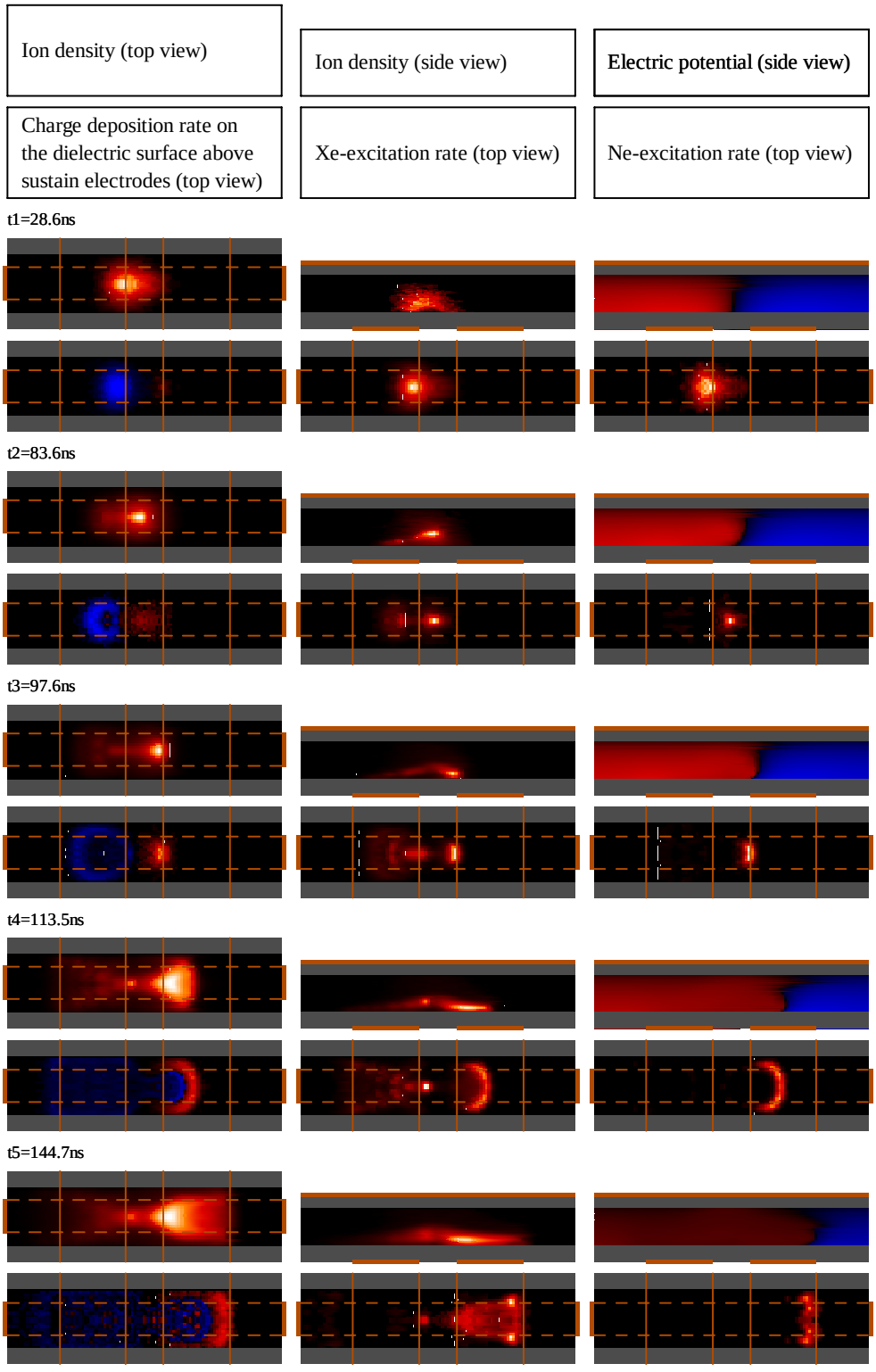

Fig.4. Spatial distribution of discharge characteristics at different moments of time. Each time-frame includes six windows whose contents are explained in the top sketch. Red color corresponds to positive values, blue – to negative ones.

Phase-1. At first, the positive charge is accumulated in the gap volume above the inner edge of the anode electrode and at the same time the negative charge is deposited on the dielectric surface. The charge created on this stage is still small and the distribution of the electric potential is almost the same as in empty gap (see Fig.4, the moment $t=t_1$).

Phase-2. Then, when the density of the positive charge reaches a certain critical level, ions starts to screen the electric field and detain the electrons in the gap volume. As a result, a plasma region forms above the inner edge of the anode and then gradually protrudes toward the cathode (see Fig.4, the moment $t=t_2$). There is a substantial positive charge on the tip of this plasma region (much like the charge on the tip of the conductor placed in an external electric field). At this stage, ongoing deposition of the negative charge on the anode dielectric surface is accompanied by the formation of first striations (see "ion density" and "Xe-excitation rate" windows in Fig. 4, the moment $t=t_2$), and the deposition of the positive charge on the cathode dielectric surface is still insignificant.

Phase-3. When the plasma region approaches the dielectric surface above the inner edge of the cathode (see Fig.4, the moment $t=t_3$), the cathode fall is formed, and the current through the low resistive plasma channel sharply increases. Since the potential drop between the plasma region and the uncharged areas of the dielectric surface is substantially higher than the breakdown voltage, the CF expands along the cathode in the form of an ionizing wave, and the positive charge is deposited on newer and newer areas of the dielectric surface. (The ionizing wave is readily identified by the red arc in "charge deposition rate", "Xe-excitation rate" and "Ne-excitation rate" windows in Fig.4, the moment $t=t_4$.) Right behind this wave, the deposition of the positive charge sharply decreases and becomes overshadowed by the deposition of the negative charge. In this area, hot electrons diffuse against (or across) the electric field from the plasma toward the surface.

Phase-4. When the positive charge covers most of the dielectric surface above the cathode (see Fig.4, the moment $t=t_5$), the discharge extinguishes. In the afterglow, the number of ions and electrons in the PDP cell gradually decreases through the dissociative recombination of electrons and Xe_2^+ molecules. Charged particles are also pulled out of the plasma toward the dielectric surfaces by the residual (and ambipolar) electric fields.

Note that the atoms of neon are excited almost exclusively in the area of the cathode (where the electric field is relatively strong), whereas the excitation of xenon atoms takes place in both anode and cathode areas (see Fig 4, Ne- and Xe-excitation rates). This difference is also observed in experimental data (see [18, 19]).

The deposition of the negative charge on the dielectric surface in the anode area initially also progresses in a wave-like manner with quite pronounced wave front of a distorted circular shape (within which the plasma striations are formed). But with time, this deposition becomes much more uniform (compare blue areas above the anode in "charge deposition rate" window in Fig. 4 at time moments t_4 and t_5 with those at time moments t_2 and t_3). In other words, with time the whole anode area gets directly involved in closing the electric circuit between the anode and the cathode.

In the next section, we describe results of specially designed numerical experiments which help us get a better understanding of physical phenomena occurring in the anode area of the PDP cell (see also a worth-while treatment [20, 21])

IV. NUMERICAL EXPERIMENTS

In the first experiment, we replace the dielectric layer above the anode by a material with high electric conductivity. In this case, the same ionizing wave propagates above the cathode, but the deposition of the negative charge occurs only within a small area above the inner edge of the anode electrode (see, Fig. 5). Now there is no component of the electric field parallel to the surface, and electrons cannot be pulled to the new surface areas; so that ionizations (and excitations) occur above the anode almost in the same place.

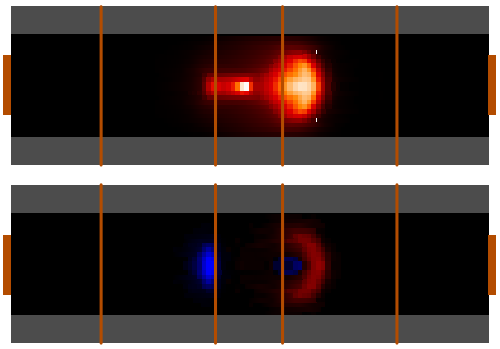

Fig. 5. Distribution of the ion density (top view) and charge deposition rate on the surface in the discharge when dielectric above the anode is replaced by a metal (red color corresponds to positive values, blue – to negative ones).

As a result, no striations occur above the metal; they can form only above dielectric surfaces, along which a non-zero component of the electric field exists.

In the second numerical experiment, we artificially make ions immobile in the left part of the PDP cell (without introducing any changes in the right part, see Fig. 6). As one can see from Fig. 6, the formation of striations is not a result

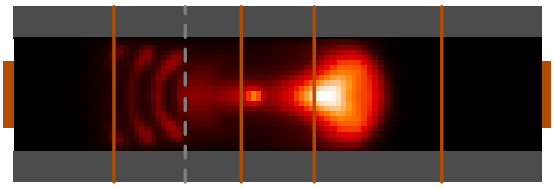

Fig. 6. Distribution of the ion density (top view) when ion velocity is artificially set to zero in the left part of the PDP cell (on the left from the dashed grey line).

of ion movements (contrary to what was suggested in [22]): "plasma stripes" near the dielectric surface become even more distinct when ion velocity is set to zero! The motion of ions in the electric field rather leads to smearing out of the spatial modulation of charged particle densities (as can be noticed in "ion density" windows in Fig. 4, the moment $t=t_5$). Overall, one can say that positively charged ions play a passive role in the considered phenomenon.

In the third experiment, we make a number of radical geometrical simplifications (see Fig. 7). In order to separate the physical phenomena near the anode from those near the cathode, we consider the formation of striations in the system composed only of an unbounded upper address electrode and

an unbounded lower anode electrode, both covered with dielectric layers (with thickness d and dielectric constant ε).

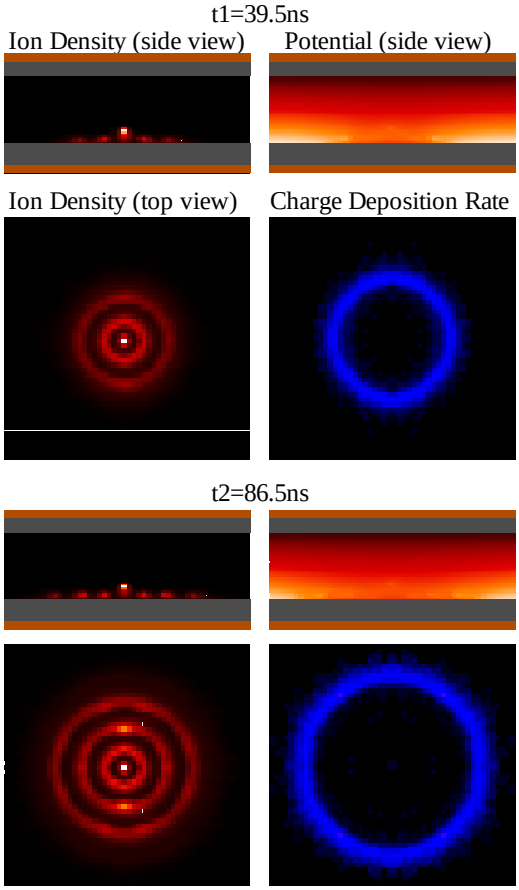

Fig.7. Spatial distribution of discharge characteristics at two moments of time in the system composed of two opposing electrodes (red color corresponds to positive values, blue – to negative ones). The position of the injection spot of electrons is identified by the brightest point in each "ion density" window.

The anode is under the positive potential V_0, so that, initially, there is only a vertical uniform electric field in the gap, $E_0=V_0/L_0$ (where L_0 is the vertical distance between address and anode electrodes). We also exclude the ion movements by setting the velocity of all the ions to zero. In order to imitate the electron source from the plasma channel in standard geometry, we inject electrons within a small area right above the surface of the anode dielectric. As one can see from Fig.7, the plasma striations and the front of the charging wave have a ring-like shape (as should be expected in the geometry without a preferred horizontal direction).

At the beginning of the injection, the electrons drift in the vertical electric field, and the negative charge is deposited on the dielectric surface right under the injection spot. With time, this negative charge reverses the vertical component of the electric field and creates its horizontal component (and a potential difference between already charged and still uncharged surface areas, as clearly seen from "potential" windows in Fig. 7). The redirected electric field pulls electrons to new areas of a bigger radius. Ions created (by the ionization processes) in the gap above the dielectric surface strongly influence the processes of transporting the electrons to uncharged areas of the surface.

Our simulations show that the result displayed in Fig. 4 is not sensitive to the time dependence of the injection current $I(t)$ (providing this current is not too strong and not to weak). The key parameter appears to be the charge Q of the time integrated current: the radius of the charging wave front (and number of striations) depends on the amount of the charge Q already deposited on the surface rather than directly on time t (in a sense, the time is excluded from our problem!). The instant velocity of the front, therefore, is controlled by the current $I(t)$.

When the distance between upper and lower electrodes is great and the thickness of the dielectric layer above the lower electrode is small, in our super simplified geometry there are only two external parameters which influence the charge deposition process: the initial electric field E_0 and the effective dielectric thickness d/ε. We have found that the smaller the latter parameter, the slower the deposition process (i.e., when we took two times smaller d/ε, we had to inject approximately two times more electrons in order to get the same striation picture).

Having tried many different energy distributions of the injected electrons and observing the same striation structure, we conclude that the results are not sensitive to the energy distribution function of injected electrons. Also, the electron losses due to elastic collisions with neutral atoms and electron-electron collisions are irrelevant for the striation phenomenon under consideration.

Analysis of simulations of the anode striations allows us to gain some insights into this phenomenon (compare to [21]): (1) Non-local effects are very important in the electron kinetics – electrons gain the energy in regions with strong electric field and lose it, via ionizations and excitations, primarily in the regions with weak electric field. (2) The negative surface charge (due to electrons deposited on the dielectric above the anode) redirects the electric field creating its longitudinal component that pulls the electrons along the dielectric surface. (3) The positive space charge (due to ions accumulated in the volume) creates a "potential channel" which retains the electrons in the volume not allowing them to escape to the dielectric surface. Thus, the electrons are transported above the surface to still uncharged areas of the dielectric surface. On their way, some of the electrons get trapped inside the potential wells of striations. (4) As the process of charging the dielectric surface above the anode involves newer areas farther and farther from the injection spot of electrons, more and more striations successively appear – so one can say that the plasma is created in the course of formation of striations, rather than striations emerge from a plasma background.

IV. CATHODE FALL SPREADING

In this section, we present some qualitative results of the study of the dynamic CF spreading along a plane cathode covered with a dielectric layer. We use the 2-dimensional

version of the PIC/MC code described in Section II. In order to avoid unnecessary complications, our system is intentionally simplified by introducing the bare anode electrode (the vertical, side electrode on the left in Fig. 8) right above the dielectric surface. By doing so, we effectively keep the plasma potential close to a constant potential of the anode (save a few volts which drop across the anode sheath). The cathode ionization wave in such a system propagates under unchanging conditions. We take neon at the pressure p=500Torr as the background gas. The vertical and horizontal dimensions of the simulation domain are taken sufficiently large (in comparison to thicknesses of the dielectric and plasma layers), so that the influence of the top and right side boundaries on the CF spreading is negligible. The thickness of the dielectric layer d is varied in different numerical experiments from 0.5μm to 100μm. The secondary emission coefficient due to ions γ=0.005-0.5. The photoemission of electrons from the surface is neglected.

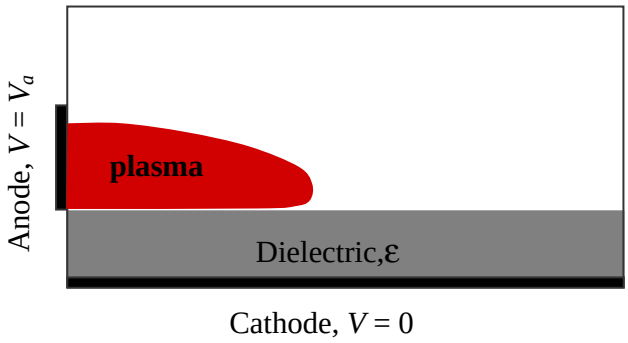

Fig. 8. Sketch of the simplified system in which the CF spreading is studied. Electrodes are shown in black; the cathode is grounded and the anode is kept under constant positive potential.

Fig. 9 illustrates the dynamics of the spreading of the CF along the dielectric layer. The parameter d/ε=10μm is taken to be close to the length of the normal DC cathode fall l_{norm}. The plasma region expands with an almost constant velocity $\mathbf{v}_f \approx 2.2$ km/s (compare top panels in both time frames in Fig.9). This velocity is of the order of the velocity of ions in the CF (maximal ion velocity in the CF $\mathbf{v}_i \approx 15$ km/s). At the chosen relationship between parameters d/ε and l_{norm}, there is a sharp boundary between charged and still uncharged areas of the dielectric surface, and the electric field is strong only in the vicinity of the tip of the plasma region (look at the bunching up of the equipotential lines in front of the tip in Fig. 9), where most of the ionizations take place. Note that in the limiting case $d/\varepsilon \to 0$ (the CF spreading over a bare metal electrode), the electric field is strong not only at the tip but everywhere under the plasma region (in the space between the plasma and the metal surface).

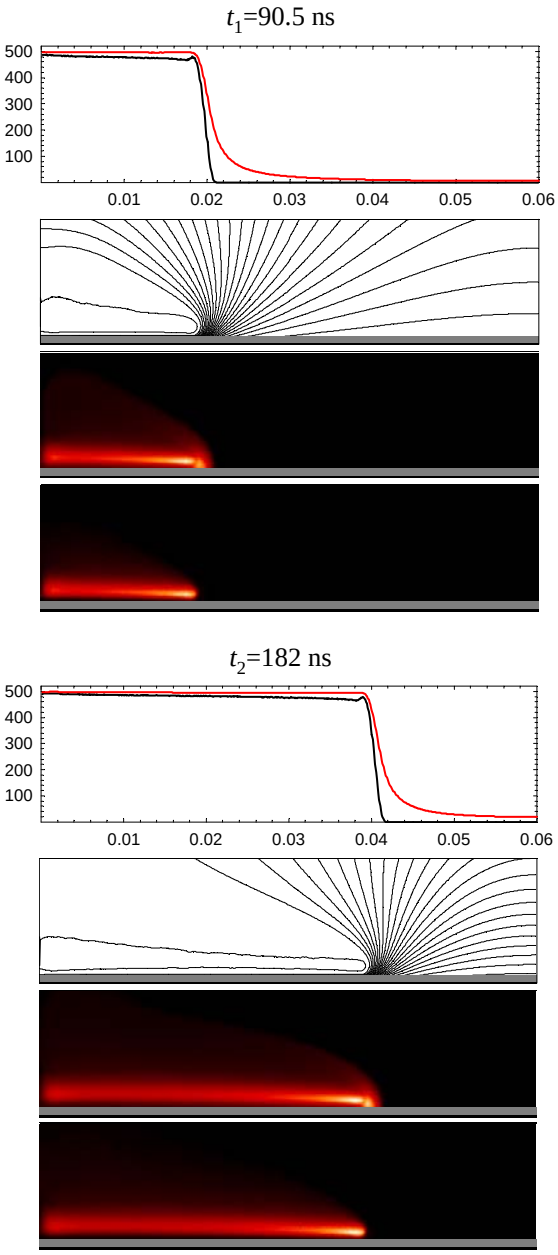

Fig. 9. Spreading of the CF above the dielectric layer; d=10μm, ε=1, V_a=500V, and γ=0.5. Top panel in each time frame shows the electric potential at the dielectric surface φ_s (dashed curve) and the renormalized surface charge σ/C (solid curve), where $C=\varepsilon\varepsilon_0/d$. The other panels show the spatial distribution of the electric potential φ (with 20V separation between the contour lines), ion density n_i, and electron density n_e in a small part of much large simulation domain; at $t=t_1$, max n_i =1.75×10^{14}cm^{-3}, max n_e =1.8×10^{14}cm^{-3}; at $t=t_2$, max n_i =1.59×10^{14}cm^{-3}, max n_e =1.59×10^{14}cm^{-3}.

It is clear that one of the necessary conditions for the CF spreading is the existence of electric field lines between the plasma region and the dielectric surface along which the production of ions in the electron avalanche exceeds their losses:

$$P_i \equiv \exp\left(\int \alpha\, dl\right) - 1 \geq \frac{1}{\gamma},$$

where the ion production coefficient P_i is the number of ions produced in an avalanche initiated by a single electron emitted from the surface, α is the electron ionization coefficient, and the integral is taken over the electric field line. A surplus of ions is left in the volume and forms (along with retained electrons) new areas of the plasma region. As the plasma region extends along the surface, the positive anode potential protrudes forward, and the electric field lines reconfigure. And then again, electron avalanches create ions and the process repeats itself. However, in contrast to a stationary CF, where the ions and electrons move along the same trajectories, it is not clear now how an ion appears at the spot where a newly created field line crosses the dielectric surface (recall that the photoemission is ignored).

A detailed study of the phenomena [12] has shown that, under typical discharge conditions, the diffusion of the electrons and ions is responsible for transporting the ions in front of the ionization wave. At the same time, the propagation of the CF also takes place if the diffusion of all the ions and electrons is purposely set to zero. But in this case the cathode wave velocity is lower, and there now exist the ion trajectories along which some ions reach the dielectric surface ahead of the spot from which the electrons that created the aforementioned ions were emitted. Interestingly, the positive charge in the front of the ionization wave is profoundly important for the existence of these special ion trajectories.

V. CONCLUSIONS

In a strong discharge in a coplanar AC-PDP cell with small distance between sustain electrodes, the physical phenomena in the cathode and anode areas weakly influence each other and connected largely by the current through the plasma channel. As the discharge develops between coplanar electrodes, it deposits the positive charge on the dielectric surface above the cathode and the negative charge on the surface above the anode. Both processes progress in a wave-like manner with quite pronounced wave fronts.

In conclusion, let us summarize the main results regarding the properties of the cathode and anode waves:

-- Propagation of the cathode ionization wave is, in essence, an expansion of the cathode fall, wherein ionization processes play a determining role. The process of charging the dielectric surface is not a driving force in the propagation of the cathode wave – it can just as easily propagate above the metal.

-- By contrast, in the anode wave the main process is deposition of the negative charge onto the dielectric surface: the deposited charge reverses the vertical component of the electric field and creates its horizontal component so that the electrons are pulled to still uncharged areas.

-- The velocity of the cathode ionizing wave is of the order of the ion velocity in the cathode fall and the diffusion of electrons and ions plays a very important role in the propagation of the cathode ionization wave.

-- The velocity of the anode charging wave is independent of the velocity of ions (and almost does not change even when ions are immobile). It is determined by the rate of the delivering of the negative charge (i.e. by the current) through the plasma channel in the area of the anode.

-- When the effective dielectric thickness d/ε decreases, the cathode ionizing wave moves faster, and the anode charging wave moves slower (so that it does not propagate at all above the bare electrode).

-- Anode striations are not sensitive to the energy distribution function of electrons coming from the plasma channel.

-- Electron losses due to elastic collisions with neutral atoms and electron-electron collisions are irrelevant for either the striation or the cathode wave propagation phenomena under consideration.

-- Non-local electron kinetics, negative surface charge, and positive volume charge above the dielectric surface are essential for the striation phenomenon.

REFERENCES

[1] D. L. Bitzer and H. G. Slottow, “The plasma display panel—A digitally addressable display with inherent memory,” in *Proc. AFIPS Conf.* Washington, DC, vol. 29, p. 541, 1966

[2] H. G. Slottow, “Plasma displays,” *IEEE Trans. Electron. Devices*, vol. 23, pp. 760-772, 1976.

[3] J. P. Boeuf, “Plasma display panels: physics, recent development and key issues,” *J. Phys. D: Appl.Phys.*, vol. 36, pp. R53-R79, 2003.

[4] S. Kawanoa and T. Misaka, “Numerical study on microdischarges in plasma display panels with arbitrary cell geometry,” J. Appl. Phys., vol. 98, p. 053302, 2005.

[5] K. Tachibana, S. Kawai, H. Asai, N. Kikuchi, and S. Sakamoto, “Characteristics of Ne–Xe microplasma in unit discharge cell of plasma display panel equipped with counter sustain electrodes and auxiliary electrodes,” *J. Phys. D: Appl. Phys.*, vol. 38, pp. 1739–1749, 2005.

[6] G. Veronis and U. Inan, “Simulation of Self-Erase Discharge Waveforms in Plasma Display Panels,” *IEEE Trans. Plasma Sci.*, vol. 33, no. 2, p. 516, 2005.

[7] Tao Jiang, M. D. Bowden, E. Wagenaars, G. M. W. Kroesen, “Emission imaging of a PDP-like microdischarge,” *IEEE Trans. Plasma Sci.*, vol. 33, no. 2, p. 506, 2005.

[8] H. G. Slottow and W. D. Petty, “Stability of discharge series in the plasma display panel,” *IEEE Trans. Electron. Devices*, vol. 18, no. 9, pp. 650-654, 1971.

[9] Yu. P. Raizer, Gas discharge physics, Berlin ; New York : Springer-Verlag, c1991.

[10] V. N. Khudik, V. P. Nagorny, and A. Shvydky, “Three-dimensional PIC/MC simulations of the sustain discharge pulse in an AC-PDP”, *Journal of the SID*, vol. 13, p. 147, 2005.

[11] V.P Nagorny and V.N. Khudik, “Three dimensional fully kinetic simulations of the discharge pulse in an AC-PDP cell”, *IDW '04*, pp. 867-870, 2004.

[12] A. Shvydky, V.N. Khudik, V.P. Nagorny, and C. E. Theodosiou, “Expansion of a Dynamic Cathode Fall along the Dielectric Surface,” 58th Gaseous Electronics Conference, Oct 16-20, 2005.

[13] R.W. Hockney and J.W. Eastwood, Computer Simulation Using Particles, IOP Publishing, Bristol, 1988.

[14] J. Meunier, Ph. Belenguer, and J.P. Boeuf, “Numerical model of an ac plasma display panel cell in neon- xenon mixtures,” *J. Appl. Phys.*, vol. 78, pp. 731-745, 1995.

[15] D. Piscitelli, A.V. Phelps, J. de Urquijo, E. Basurto, and L.C. Pitchford, “Ion mobilities in Xe/Ne and other rare-gas mixtures,” *Phys. Rev. E*, vol. 68, p. 046408, 2003.

[16] S. Rauf and M. J. Kushner, “Dynamics of a coplanar-electrode plasma display panel cell. I. Basic operation,” *J. Appl. Phys*., vol. 85, p. 3460, 1999.

[17] C. K. Birdsall and A. B.Langdon, Plasma physics via computer simulation, Bristol, Eng.: Adam Hilger, c1991.

[18] L.F. Weber, “Status and trends of plasma display device research,” unpublished results presented at the International Display Research Conference (EuroDisplay'99), Berlin, Germany, Sept. 1999.

[19] A complete movie of the time evolution. [Online]. Available: http://www.plasmadynamics.com.

[20] C.H. Shon and J.K. Lee, “Striation phenomenon in the plasma display panel,” *Phys. Plasmas*, vol. 8, pp. 1070 – 1080, March 2001.

[21] F. Iza, S. S. Yang, H. C. Kim, and J. K. Lee, “The mechanism of striation formation in plasma display panels,” *J. Appl. Phys.*, vol. 98, p. 043302, 2005.

[22] G. Cho, E. H. Choi, Y. G. Kim, D. I. Kim, H. S. Uhm, Y. Yoo, J. G. Han, M. C. Kim, and J. D. Kim, “Striations in a coplanar ac-plasma display panel,” *J. Appl. Phys.*, vol. 87, pp. 4113-4118, 2000.